

RESEARCH PAPER

In-chirp FSK communication between cooperative 77-GHz radar stations integrating variable power distribution between ranging and communication system

WERNER SCHEIBLHOFFER¹, REINHARD FEGER¹, ANDREAS HADERER², STEFAN SCHEIBLHOFFER³
AND ANDREAS STELZER¹

We present the realization of a cooperative radar system for ranging applications with integrated data-transmission capability. The simultaneous transmission is performed by the radar-hardware without the necessity of additional components or an auxiliary data-link. Therefore, the data are directly embedded in the transmitted chirp of a frequency-modulated continuous-wave radar sensor. A second station, acting as receiver, uses an identical, but unmodulated chirp for down-conversion. The resulting signal then is processed by a non-coherent demodulator setup, extracting the communication data. Measurement results from transmission of messages with different bit-rates are shown. By utilizing existing radar-hardware a transmission rate of up to 256 kbps is possible, without the need of a dedicated transceiver. Additionally, a method to optimize the ranging results by variable distribution of the available signal power between distance-measurement and communication system is presented.

Keywords: Microwave measurements, Radar architecture and systems, Cooperative systems

Received 15 October 2015; Revised 18 December 2015; Accepted 28 December 2015; first published online 12 February 2016

I. INTRODUCTION

The fourth industrial revolution is based on cyber-physical systems, where communication between different clients such as roboters and handlers, as well as the produced good itself is a crucial factor. The implementation of the communication task necessary for interaction and data-exchange between these clients is often based on microwave systems. Additionally, advanced, contact-less sensors are finding their way into automated production sites. While optical systems are widespread, the number of microwave-based radar sensors is increasing, because they are suitable for operation in harsh environmental conditions such as dust or rough weather. It could be shown that latter systems can be operated in cooperative modes [1] gaining an additional advantage over conventional measurement approaches. A ranging-system based on the dual-ramp frequency-modulated continuous-wave (DR-FMCW) principle, which uses a dedicated external communication-link, has been presented in [2]. In a multi-

sensor system this link can be used to select different pairs of clients for distance measurements, to retrieve data, or the unique identification codes from the selected clients. Based on the above principle a novel method for directly embedding a data-link into the transmit chirp of a frequency-modulated continuous-wave (FMCW) radar is presented. This implementation eliminates the need for dedicated data-transmission timeslots between the chirps [3], increasing the measurement rate as well as the real-time capability of the whole system. This contribution is an extended version from [4]. Compared with this it discusses the crucial parameters and generation of the transmit signal with the onboard hardware in detail. A modified receiver design, better suitable for implementation in hardware signal-processing units for digital demodulation is introduced. Furthermore, hardware limitations for the maximum possible data-rate are derived and a method to assure the outstanding ranging-performance of the system, while applying data-transmission on the ramp is shown.

II. MEASUREMENT AND COMMUNICATION PRINCIPLES

For the implementation of the communication-link a system, based on the classical FMCW radar principle [5] is used. It is capable to operate in the cooperative DR-FMCW

¹Institute for Communications Engineering and RF-Systems, Johannes Kepler University Linz, Altenbergerstr. 69, Linz, A-4040, Austria. Phone: +43 732 2468 6376

²Inras GmbH, Altenbergerstr. 69, A-4040 Linz, Austria

³Hainzl Industriesysteme GmbH, Industriezeile 56, A-4030 Linz, Austria

Corresponding author:

W. Scheiblhofer

Email: w.scheiblhofer@nthfs.jku.at

measurement mode, where multiple stations interact to obtain the respective distance information. The measurement setup consists of i stations, using linear frequency sweeps with identical chirp-rates $k = B_{sw}/T_{sw}$ as transmit signal. The sweep bandwidth B_{sw} is covered within the ramp-duration T_{sw} , depicted in Fig. 1. After a predefined coarse temporal pre-synchronization with μs accuracy, station one immediately starts to transmit its chirp, which is received at station two after the additional time-of-flight (TOF) τ . The start of the sweep at the second station is delayed by the adjustable parameter T_{off} . The received signal at each station is down-converted with a copy of the local transmit (TX) signal from the other station. The range information then can be calculated from the combined information of the participating sensor nodes, thus presuming a data-link [6].

The existing microwave link can be used for data-exchange purposes as well, e.g. by the superposition of a conventional modulation technique with the frequency chirp. In [7], a concept of amplitude modulation is presented to enhance a classical FMCW radar system with the ability to send data to specially designed receivers. In [8], an analysis of the combined waveform of frequency-shift keying (FSK) and linear frequency modulation, using up- and downchirps for communication and distance measurement, respectively is given. In [9], a specially designed direct digital synthesis (DDS)-based hardware-realization is used for characterization in a laboratory. In contrast to this, a data-link, based on the FSK modulation technique is directly implemented to cooperative 77-GHz radar-stations in the presented setup at hand. This link is then used to perform the exchange of the measurement data. The values of single symbols are represented as unique frequencies $f_{mod,m}$ where the integer m denotes the index of the related modulation signals. This m signal waveforms of the FSK modulation can be expressed as

$$s_{mod,m}(t) = A_{mod,m} \cos(2\pi f_{mod,m}t + \varphi_{mod,m}) + a_{dc,mod,m}, \quad (1)$$

where $A_{mod,m}$ is the signal magnitude, $\varphi_{mod,m}$ the initial phase, and $a_{dc,mod,m}$ a constant offset. A schematic of the transmitter is depicted in Fig. 2.

Prior to transmission, the linearly frequency-modulated signals of the participating sensor nodes can be described as

$$s_{LO,i}(t) = A_{LO,i} \cos\left(2\pi\left(f_{o,i}t + \frac{k}{2}t^2\right) + \varphi_{o,i}\right). \quad (2)$$

Here $A_{LO,i}$ denotes the magnitude, $f_{o,i}$ the start frequency, and $\varphi_{o,i}$ the initial phase of the transmitted chirp, which is identical to the local oscillator (LO) signal before modulation.

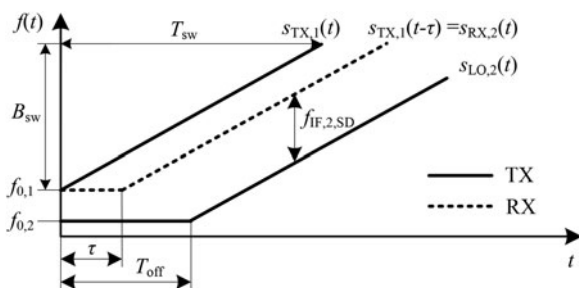


Fig. 1. Frequency chirps relevant for the second station of the DR-FMCW cooperative radar.

Assuming the sensor node with $i = 1$ as transmitting station, the up-conversion of $S_{mod,m}(t)$ with $s_{LO,1}(t)$ results in $S_{TX}(t)$ as

$$\begin{aligned} s_{TX,1}(t) &= s_{LO,1}(t)s_{mod,m}(t) \\ &= A_{TX,1} \left(\cos\left(2\pi\left(f_{o,1}^+t + \frac{k}{2}t^2\right) + \varphi_{o,1}^+\right) \right. \\ &\quad \left. + \cos\left(2\pi\left(f_{o,1}^-t + \frac{k}{2}t^2\right) + \varphi_{o,1}^-\right) \right) \\ &\quad + A_{dc} \cos\left(2\pi\left(f_{o,1}t + \frac{k}{2}t^2\right) + \varphi_{o,1}\right), \end{aligned} \quad (3)$$

where the abbreviations $A_{TX,1} = A_{LO,1}A_{mod,m}/2$, $A_{dc} = A_{LO,1}a_{dc,mod,m}$, $f_{o,1}^+ = f_{o,1} + f_{mod,m}$, $f_{o,1}^- = f_{o,1} - f_{mod,m}$, $\varphi_{o,1}^+ = \varphi_{o,1} + \varphi_{mod,m}$, and $\varphi_{o,1}^- = \varphi_{o,1} - \varphi_{mod,m}$ were used. Note, that without loss of generality, only a single bit value was considered at the up-conversion process, for sake of simplicity. After the TOF τ , determined by the distance R between the participating sensor nodes, the delayed version of $S_{TX,1}(t)$ is impinging on the receiving station as $S_{RX,2}(t)$. The corresponding LO signal generated by the second sensor node, as shown in Fig. 2, is also delayed by the offset time T_{off} resulting in

$$\begin{aligned} s_{RX,2}(t) &= s_{TX,1}(t - \tau) \\ s_{LO,2}(t) &= s_{LO,1}(t - T_{off}) \\ &= A_{LO,2} \cos\left(2\pi\left(f_{o,2}(t - T_{off}) \right. \right. \\ &\quad \left. \left. + \frac{k}{2}(t - T_{off})^2\right) + \varphi_{o,2}\right). \end{aligned} \quad (4)$$

The subsequent down-conversion results in the intermediate frequency (IF) signal

$$\begin{aligned} s_{IF,2}(t) &= s_{LO,2}(t)s_{RX,2}(t) \\ &\approx A_{IF,2} \cos\left(2\pi\left(f_{R,m}^+t + \varphi_{o,IF}^+\right) \right) \\ &\quad + A_{IF,2} \cos\left(2\pi\left(f_{R,m}^-t + \varphi_{o,IF}^-\right) \right) \\ &\quad + A_{IF,R} \cos\left(2\pi f_R t + \varphi_{o,R}\right) \end{aligned} \quad (5)$$

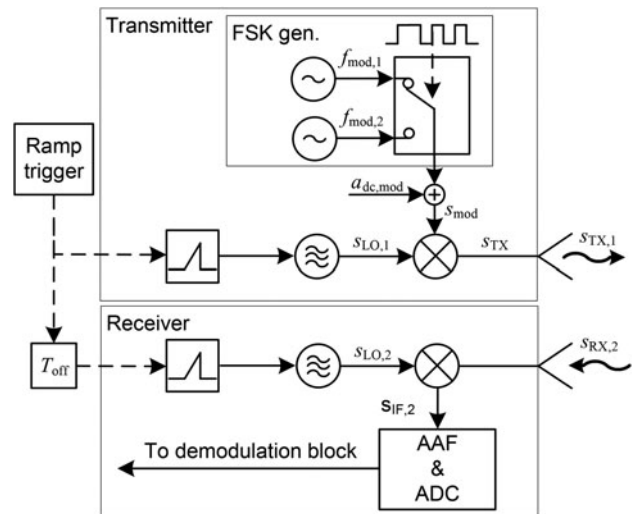


Fig. 2. Block schematic of the transmitter, generating the FSK-modulated FMCW chirp and the receiver.

with $f_{R,m}^+ = f_R + f_{\text{mod},m}$, $f_{R,m}^- = f_R - f_{\text{mod},m}$, and the signal magnitudes

$$A_{\text{IF},2} = A_{\text{LO},1} A_{\text{LO},2} A_{\text{mod},m} / 4, \quad (6)$$

$$A_{\text{IF},R} = A_{\text{LO},1} A_{\text{LO},2} a_{\text{dc},\text{mod},m} / 2. \quad (7)$$

Constant phase-terms have been summarized by $\varphi_{0,\text{IF}}^+$, $\varphi_{0,\text{IF}}^-$, and $\varphi_{0,R}$. The frequency f_R is the relevant signal component for the ranging system [6] with

$$f_R = (f_{0,2} - f_{0,1}) + k(T_{\text{off}} - \tau). \quad (8)$$

In addition to the frequency components caused by f_{mod} , which carry the data-information, two frequency terms can be observed in (8). The first one results from the offset between the starting frequencies $f_{0,i}$ of the ramp. The second term includes the range dependency between the stations, expressed by TOF τ . Due to the coarse temporal pre-synchronization of the stations and dependency of the latter term from the distance, the resulting frequency is not known exactly. Nevertheless the modulation frequencies $f_{\text{mod},m}$ are centered symmetrically around f_R . A crucial factor for the demodulation within the receiver, described in the following section, is the existence of the ranging-signal in the IF signal. This can be achieved by setting $a_{\text{dc},\text{mod},m} \neq 0$ in (1).

A) Construction of the transmit signal

To design an ideal FSK TX signal used for the on-ramp data-link, several characteristics of the transmitter and receiver have to be taken into account to optimize the communication concerning high transmission rate and low bit-error rate. One of these conditions is the orthogonality criterion: The different chosen modulation signals should not interfere with each other during the detection process, thus they have to be uncorrelated [10]. This subsequently leads to the orthogonality condition for the different frequency components $f_{\text{mod},m}$ of (1) with

$$f_{\text{mod},m} = \frac{m}{T_{\text{sym}}},$$

$$\Delta f_{\text{mod}} = f_{\text{mod},m+1} - f_{\text{mod},m} = \frac{1}{T_{\text{sym}}},$$

where T_{sym} is the duration of a single symbol. The transmitted signal can be generated by switching between these frequencies. In general, this would lead to discontinuities at the transition between different bit-states, broadening the spectral signal bandwidth. To avoid interferences between different radar and communication systems, federal regulations concerning the useable bandwidth have to be fulfilled. This means that a continuous phase in the FSK signal is desired, leading to the continuous-phase FSK [11]. Although not implemented in the current approach, the data stream can additionally be shaped with Gaussian filters to further reduce the required bandwidth, but this potentially increases the probability for intersymbol interference (ISI) due to overlapping bit edges [12]. The latter method called Gaussian minimum shift keying (GMSK) is applied at the global system for mobile

communications (GSM) system for cellular phones and uses sophisticated methods for bit error correction e.g. the Viterbi algorithm [13] to get rid of the ISI. A further key parameter is represented by the maximum possible sample rate f_s of the used analog-to-digital converter (ADC) at the receiving station. Assuming, that the ranging frequency at the receiver can be centered at $f_R = f_s/4$, this leads to the restriction for the highest used modulation frequency

$$f_{\text{mod},m_{\text{max}}} < f_s/2 - f_R = f_s/4.$$

Extending the communication-link to an M -ary FSK modulation scheme enables the transmission of multiple bits with a single symbol at once. While M increases, the given probability of a bit error decreases asymptotically to the Shannon limit [10], while the need for additional modulation frequencies $f_{\text{mod},m}$ increases the necessary bandwidth. To minimize the influence of the sidelobes from the data-link for the ranging signal, a minimum offset of 200 kHz of the first FSK frequency from f_R is chosen. According to these boundaries and referring to the system parameters in Section II, the presented system is able to operate with a 16FSK modulation scheme, transmitting four bits in a single symbol.

B) Variation of amplitude and DC-offset

A digital binary phase-shift keying modulator, integrated into the transmitter, enables the frontend (FE) to switch the phase of the outgoing signals by $\Delta\varphi = 180^\circ$ [14]. This modulator, clocked with $f_{\Delta\Sigma} = 80$ MHz, multiplies $S_{\text{LO},1}(t)$ with a ± 1 sequence to generate the desired analog modulation frequency f_{mod} . A positive characteristic of such a $\Delta\Sigma$ modulator is that the quantization noise is suppressed at lower frequencies by shifting the noise power toward higher frequencies. Thus, noise components, introduced by the $\Delta\Sigma$ modulator, can be filtered out. This can be optimized by the selection of the parameter set of the $\Delta\Sigma$ modulator, the FMCW parameters and f_{mod} . In contrast to using separate oscillators for generation of the different $f_{\text{mod},m}$, this modulator approach gives the remarkable advantage to completely digitally synthesize a phase-continuous M -ary FSK transmit signal. Additionally the vital parameters for the ranging system $a_{\text{dc},\text{mod},m}$ and $A_{\text{mod},m}$ in (3) can be digitally controlled. While $a_{\text{dc},\text{mod},m}$ directly influences the magnitude of the ranging signal f_R , see (5), this parameter cannot arbitrarily be increased, as the $\Delta\Sigma$ modulator cannot add any power to the outgoing signal. This means that the absolute maximum amplitude of (1) is limited to one and a tradeoff between $a_{\text{dc},\text{mod},m}$ and $A_{\text{mod},m}$ has to be found. Furthermore it is preferred that the ranging signal represents the dominant spectral component, which requires $A_{\text{IF},2} < A_{\text{IF},R}$, as this simplifies the demodulation. From (6) and (7) the subsequent conditions can be found to be

$$\begin{aligned} A_{\text{mod},m} &\leq 1 - a_{\text{dc},\text{mod},m}, \\ A_{\text{mod},m} &< 2a_{\text{dc},\text{mod},m}, \end{aligned}$$

which can be translated to

$$\begin{aligned} 0 &\leq A_{\text{mod},m} \leq 0.66, \\ \frac{A_{\text{mod},m}}{2} &\leq a_{\text{dc},\text{mod},m} \leq 1. \end{aligned}$$

Obviously this opens up an additional degree of freedom, where the signal power between the ranging and the communication signal can be distributed toward each other like it is depicted in Fig. 3, depending on the preferred operation mode. If ranging is the prioritized function of the measurement system it is desired to maximize the power level of the carrier signal while maintaining just enough energy for the data-transmission.

III. DEMODULATION

The presented demodulation system is based on a non-coherent detection approach, where the phase of the carrier does not need to be determined exactly. In contrast to coherent demodulation and detection techniques, the estimation of the m carrier phases can be avoided [10]. This is advantageous for the presented implementation, since the data is transmitted on an FMCW chirp with non-perfect linearity, potentially causing unmodeled phase deviations during the sweep. Compared with coherent demodulation with a theoretical data-rate of $bps = 2\Delta f_{mod}$ for the non-coherent demodulation the data-rate is lowered to $bps = \Delta f_{mod}$, but the complexity of the receiver architecture is significantly reduced, at nearly the same bit-error rate (BER) [15]. Figure 4 shows the implementation of the realized simple, but effective data-demodulation circuitry. The receiver only needs information about the parameters of the FSK signal, used for data-transmission. These are the overall transmission rate $bps = 1/T_{sym}$ and the used modulation frequencies $f_{mod,m}$.

The demodulation procedure starts at the end of every chirp, when the complete IF signal has been acquired. Under the assumption, that the ranging signal is the dominant spectral component, its frequency f_R can be determined by a discrete Fourier-transformation (DFT). Then S_{IF} is downconverted to zero-IF with respect to f_R by a mixer prior to further demodulation, resulting in the new base-function $S_{IF,base}$. Independent from the ranging frequency f_R , which varies from measurement to measurement, the components in the next steps can be properly designed with fixed parameters. For every transmitted symbol a spectrally matched narrow-band bandpass-filter (BPF) with the center frequency $f_{BB,m} = f_{mod,m}$ can now be applied to extract the frequency-regions where the data-information is expected, resulting in $S_{BB,m}$. Consecutive envelope detectors compare the magnitudes of the envelopes, integrating the values in the sampling region of $T_{sym}/4$ to $3T_{sym}/4$. The limitation of the sampling region ensures that the bit-transition

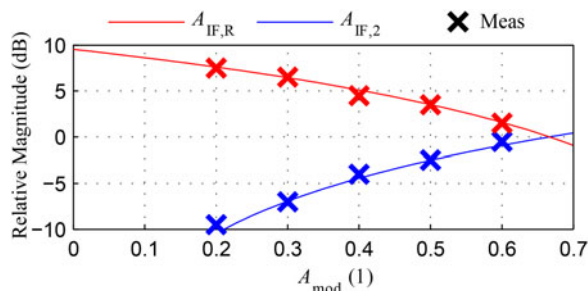


Fig. 3. Distribution of the signal power between ranging- and communication signal. As reference the maximum power for the communication signal with $A_{mod} = 0.66$ is chosen.

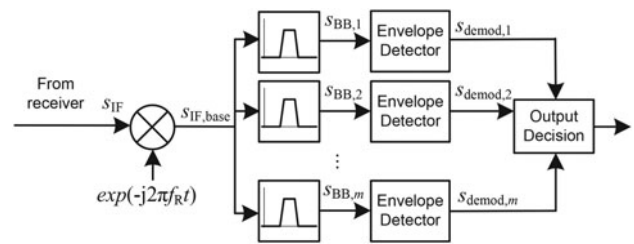


Fig. 4. Schematic of the implemented non-coherent FSK demodulation circuitry.

regions are excluded and the values are evaluated in their steady state only. For optimum detection results the 3 dB cut-off frequency of the low-pass filters of the envelope detection circuits is chosen to vary directly with the keying speed [16]. A fact that also should be taken care of is the possibility of different chirp rates caused by independent crystal oscillators for the generation of the ramp as well as the communication signal. Even if the difference is in the region of some ppm, which is typical for industrial crystal oscillators, the difference can cause a drift of the carrier frequency during the chirp of the order of several 10 kHz as it could be shown in [6]. The bandwidth of the BPF is therefore slightly extended to cover this drift. The output decision compares the envelope detector output and forwards the corresponding digitized symbol representation to the receivers output. The results are stored for consecutive calculation of the BER.

IV. MEASUREMENT SETUP

A) Hardware

The main components of the presented system’s sensor nodes are the radar FE and baseband board, depicted in Fig. 5. The 77-GHz FE uses integrated multi-channel SiGe-based TX and receive (RX) chips [17]. To generate a broadband linear frequency sweep the transmitter’s voltage-controlled oscillator (VCO) is stabilized by a phase-locked loop (PLL) with an integrated fractional-N synthesizer. A 12-bit ADC is used for digitizing the IF signal after low-pass filtering. For BB processing an Nvidia® Tegra® CPU combined with an Altera® Cyclone III FPGA is used. The multichannel system can be

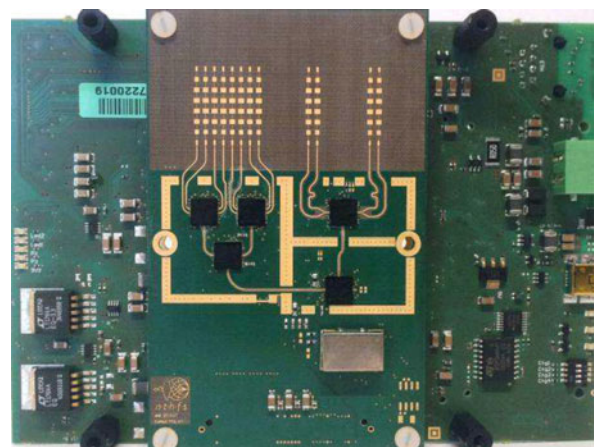


Fig. 5. Photograph of the 77-GHz radar sensor.

used in a direction-of-arrival approach to determine the relative angle of the stations to each other, as it was shown in [18]. The measurements have been conducted in a radar measurement chamber, as depicted in Fig. 6.

B) Data-rate considerations

For normal operation of the cooperative radar system at hand, it is valid to transmit the spectral position of the ranging-signal with a 32-bit value. With respect to future implementations of a communication protocol, an optional block for overhead-data with 16 bit is also provided. A cyclic-redundancy check block with a length of 16 bits is generated and appended to the data, enabling the receiving station to verify the correctness of the incoming data. To completely eliminate the timeslots used for data-transmission between the chirps, these 64 bit have to be transferred on a single sweep with the duration of $T_{sw} = 0.5$ ms, resulting in a necessary transmission rate of $bps = 128$ kbps. Following the rules, derived in Section II, the upper limit for the transmission rate is a 16FSK modulation scheme at a symbol rate of $f_{sym} = 64$ kHz, achieving a gross data-rate of 256 kbps. The modulation frequencies are then placed at $f_{mod,0} = 256$ to $f_{mod,15} = 1216$ kHz with $\Delta f_{mod} = 64$ kHz. The same data-rate at reduced necessary bandwidth can also be realized by $f_{sym} = 128$ kHz and 4FSK modulation, where $f_{mod,0} = 256$ to $f_{mod,15} = 640$ kHz with $\Delta f_{mod} = 128$ kHz.

V. MEASUREMENT RESULTS

The principle of FSK data-transmission has been evaluated by several test-measurements with data-rates between 32 and 256 kbps. The distance between the sensor nodes of the cooperative DR-FMCW measurement system was set to five meters to establish a reproducible measurement scenario, as it can be seen in Fig. 6. One node was used as transmitter, whereas the second node was used as receiver only for the communication tests. To generate comparable results the ramp-parameters and the modulation parameters, noted in Table 1 have been set identical for every measurement. The distance measurement was performed at distances between 1 and 5 m, comparing measurements with and without data on the FMCW ramp. As it was shown in [19], the phase noise is the dominant source of noise for cooperative radar systems. Thus, even when the overall signal power decreases

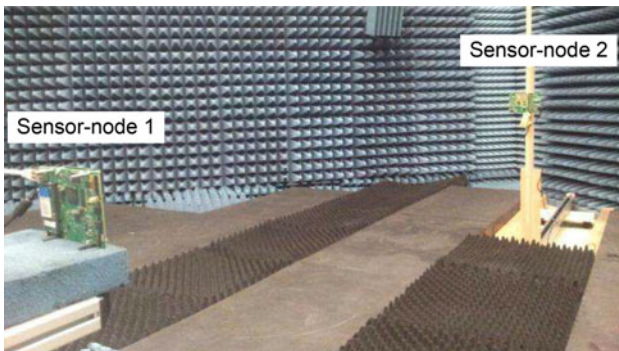


Fig. 6. Setup of the measurement in the radar measurement chamber with the two cooperative sensor nodes.

Table 1. System- and measurement parameters.

Start frequency f_o	77 GHz
Bandwidth B_{sw}	1 GHz
Ramp duration T_{sw}	0.5 ms
Offset time T_{off}	400 ns
ADC sampling rate f_s	6.667 MS/s
$\Delta\Sigma$ modulator sample rate $f_{\Delta\Sigma}$	80 MHz

at higher distances, the signal-to-noise ratio (SNR) stays nearly identical, which can also be seen from Fig. 7, comparing the relation of the ranging-peaks to the noise-floor. This characteristic is typically valid for the interesting distances up to 100 m for the system at hand.

A) Communication system

Figure 7 shows the comparison of a spectrum of the IF signal $S_{IF,2}$ with a 2FSK- and without data-modulation, where $A_{mod} = 0.5$ was set. As expected, the power level of the ranging frequency f_R decreases for the signal with additional communication data, as a portion of it is distributed to the spectral components at $f_R \pm f_{mod,m}$.

In Fig. 8, an FMCW IF-signal prior demodulation, superposed with the implemented data-transmission is depicted. The chirp is segmented into equidistant portions of the corresponding bit-length at the transmission of a binary 32-bit and a 16FSK message, each with $f_{sym} = 64$ kHz. The FSK modulation scheme, as well as the binary data-vector itself can be clearly identified. The normalized signals from the 32-bit dataset, $S_{BB,m}$ and $s_{demod,m}$ are shown in Fig. 9. Here the results from the application of the described demodulation procedure are compared with the originally transmitted bit-vector. For improved visualization, the graphs representing the bits with value 0 and the corresponding signals are inverted in polarity. The output of the demodulator has been compared with the randomly generated bitstreams, transmitted during these measurements.

To achieve a meaningful BER, 10 million bits have been transmitted for different settings of the communication system each. The results of the evaluated points and the outcome of according simulations are depicted in Fig. 10. To maintain comparability between different symbol rates,

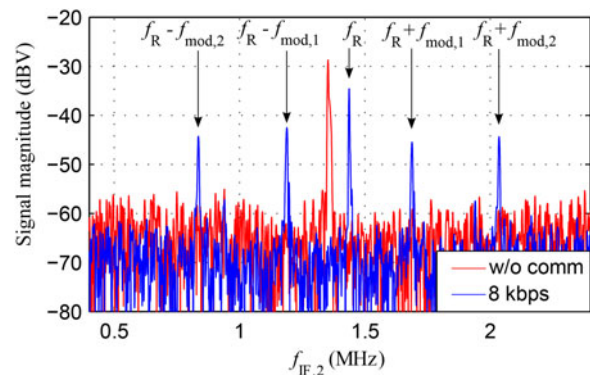


Fig. 7. Comparison of the IF spectrums of the entire ramp within the receiving station with (blue) and without (red) FSK-modulated TX signal at identical distance. The carrier at f_R and two exemplary tones at an offset of $f_{mod,1} = 250$ and $f_{mod,2} = 600$ kHz can be seen on both sides of the carrier signal. The magnitude of the communication signal was chosen to be $A_{mod} = 0.5$.

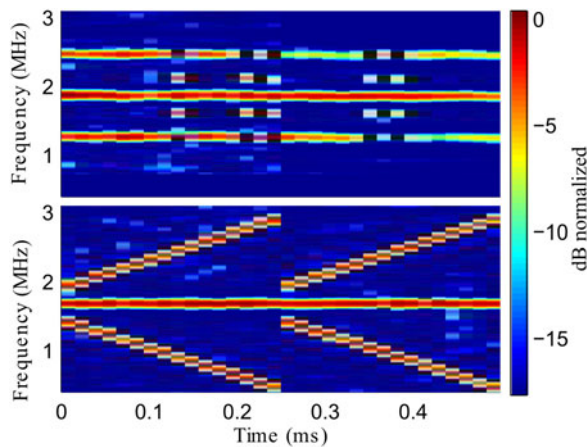


Fig. 8. Visualization of the frequency components of the segmented IF signal around f_R . Top: random 32-bit random test message. Bottom: 16FSK test message at $f_{sym} = 64$ kHz.

the SNR axis is referring to the signal power of the communication signal. It is in direct relation to the power of the ranging signal by $A_R = 2A_{IF,2d_{dc,mod}}/A_{mod}$ derived from, e.g. (6) and (7). In Fig. 10, the outcome of the measurement for the communication system is depicted, with the transmission rates of $bps = 256$ and $bps = 128$ kbps. As expected the error rate increases with rising symbol rates, as the energy per symbol decreases due to their shorter temporal length. In contrast to this, the error-rate for the M -ary FSK transmissions lies below the error rate for the binary FSK transmission. To achieve the same transfer rate higher-order M -ary FSK modulation schemes take advantage of longer T_{sym} at cost of higher spectral bandwidth occupancy. The ability to vary the power distribution between communication- and ranging signals therefore enables us to maximize the SNR for the distance measurement. This is done by choosing a reasonable BER and accordingly limiting the power for the communication signal. The impact of the variation of A_{mod} can be seen in the bottom part of Fig. 10. There, the markers representing

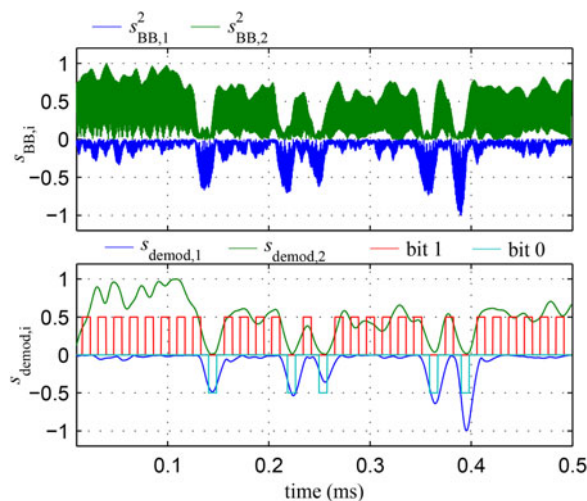


Fig. 9. Normalized signals $s_{demod,i}$ and the corresponding transmitted detection regions for a 32-bit random test message. On top the squared $s_{BB,i}$ signals within the envelope detector are depicted, whereas on the bottom the detectors output is shown. For improved visualization the graphs representing bit 0 are inverted in polarity.

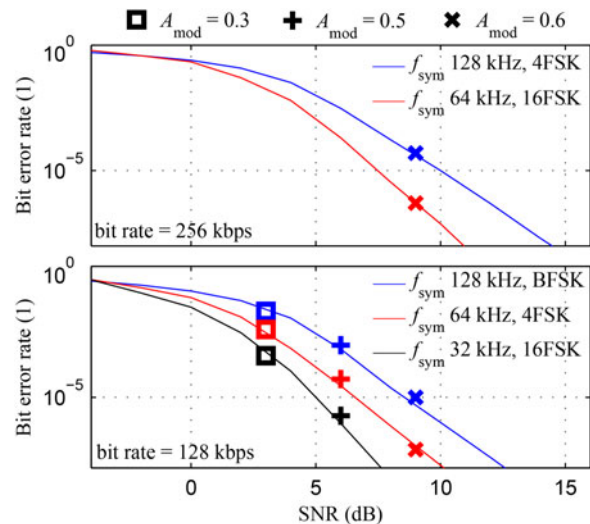


Fig. 10. Measured (markers) and simulated (lines) BER for different symbol rates, M -ary FSK and A_{mod} over SNR for ranging signal. Top: Outcomes for the maximum possible transmission rate of $bps = 256$ kbps. Bottom: Outcome for the necessary bitrate of $bps = 128$ kbps.

the measurement results depict an increasing BER, caused by reduction of A_{mod} .

B) Ranging system

Results from the distance evaluation are depicted in Fig. 11, comparing the influence of the data-transmission on the ramp with conventional DR-FMCW measurements. Additionally the influence of the variation of the magnitude of the communication signal A_{mod} is depicted for a communication signal with $f_{sym} = 32$ kHz and 16FSK. The system achieved the expected performance for the measurement without communication. The reduced power of the spectral peak of the ranging signal leads to the expected rising of the standard-deviation, but this effect can be significantly reduced by the variable power distribution.

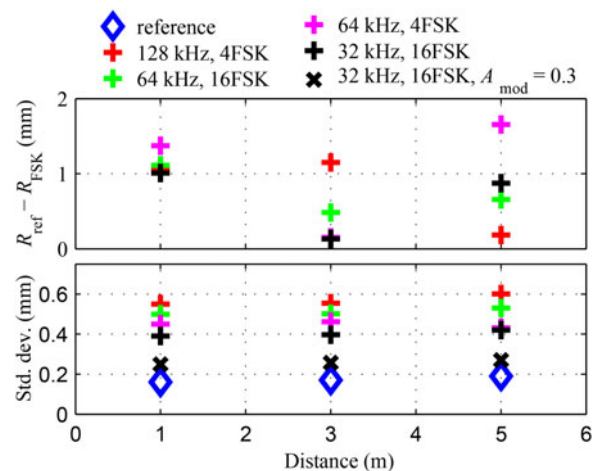


Fig. 11. Top: Range deviation of an FMCW reference measurement to measurements with data-transmission. Bottom: standard deviation of the standard deviation for the conducted measurements. The magnitude of the ranging signal is set to be $A_{mod} = 0.6$, while a measurement with $A_{mod} = 0.3$ for $f_{sym} = 32$ kHz and 16FSK is also depicted for comparison.

VI. CONCLUSION

In this paper, we presented the successful implementation of a data-link between sensor nodes of the 77-GHz DR-FMCW radar system, using the existing hardware resources. It was shown, that the superposition of a conventional modulation technique with the frequency chirps of cooperative FMCW sensor nodes can be used for communication purposes, without the need of dedicated transceiver hardware. The actual concept proves the capability of transmission-rates up to 256 kbps while maintaining the outstanding ranging-performance of the measurement system. Additional, a method to optimize the ranging results, while maintaining a constant BER by flexible distribution of the available power between the distance measurement and communication system has been shown. The integration of the data link on the FMCW ramp is an important new feature for the whole cooperative measurement system, pointing out its multi-purpose capability. The eliminated need for dedicated time slots for data-transmission can be used to increase the real-time capability of the system.

ACKNOWLEDGEMENTS

This work has been supported by the Linz Center of Mechatronics (LCM) in the framework of the Austrian COMET-K2 program and DICE GmbH & Co KG, part of Infineon.

REFERENCES

- [1] Roehr, S.; Gulden, P.; Vossiek, M.: Precise distance and velocity measurement for real time locating in multipath environments using a frequency-modulated continuous-wave secondary radar approach. *IEEE Trans. Microw. Theory Tech.*, **56** (10) (2008), 2329–2339.
- [2] Stelzer, A.; Jahn, M.; Scheibelhofer, S.: Precise distance measurement with cooperative FMCW radar units, in *IEEE Radio and Wireless Symp.*, January 2008, 771–774.
- [3] Moghaddasi, J.; Wu, K.: Improved joint radar-radio (radcom) transceiver for future intelligent transportation platforms and highly mobile high-speed communication systems, in *2013 IEEE Int. Wireless Symp. (IWS)*, April 2013, 1–4.
- [4] Scheibelhofer, W.; Feger, R.; Haderer, A.; Stelzer, A.: Method to embed a data-link on FMCW chirps for communication between cooperative 77-GHz radar stations, in *Proc. European Microwave Conf.*, September 2015, 181–184.
- [5] Stove, A.G.: Linear FMCW radar techniques. *IEE Proc. F. Radar Signal Processing*, **5** (139) (1992), 343–350.
- [6] Scheibelhofer, W.; Scheibelhofer, S.; Schrattecker, J.O.; Vogl, S.; Stelzer, A.: A high-precision long-range cooperative radar system for gantry rail crane distance measurement. *Int. J. Microw. Wirel. Technol.*, **7** (3–4) (2015), 479–487.
- [7] Barrenechea, P.; Elferink, F.; Janssen, J.: FMCW radar with broadband communication capability, in *Proc. European Microwave Conf.*, October 2007, 130–133.
- [8] Chen, X.; Wang, X.; Xu, S.; Zhang, J.: A Novel Radar Waveform Compatible with Communication, in *2011 Int. Conf. on Computational Problem-Solving (ICCP)*, 177–181.
- [9] Liu, Z.; Zhang, W.; Xu, S.: Implementation on the Integrated Waveform of Radar and Communication, in *2013 Int. Conf. on Communications, Circuits and Systems (ICCCAS)*, 200–204.
- [10] Proakis, J.G.; Salehi, M.: *Communication Systems Engineering*, 2nd ed., Prentice Hall, Upper Saddle River, NJ, 2002.
- [11] M. P. Mullo and MASSACHUSETTS INST OF TECH LEXINGTON LINCOLN LAB., A Multi-level Phase Continuous Fsk Modulator. M.I.T. Lincoln Laboratory, 1969. [Online]. Available: <https://books.google.at/books?id=MwzhHAAACAAJ>
- [12] Mouly, M.: *The GSM System for Mobile Communications: A Comprehensive Overview of the European Digital Cellular Systems*, Cell & Sys, Palaisu, France, 1992.
- [13] Benelli, G.; Farzelli, A.; Salvi, F.: Simplified Viterbi processors for the GSM Pan-European cellular communication system. *IEEE Trans. Veh. Technol.*, **43** (4) (1994), 870–878.
- [14] Feger, R.; Ng, H.; Pfeffer, C.; Stelzer, A.: A delta-sigma transmitter based heterodyne FMCW radar, in *Proc. 10th European Radar Conf.*, Nuremberg, DE, 10 2013, 208–211.
- [15] Smith, D.R.: *Digital Transmission Systems*. Springer US, 2012. [Online]. Available: <https://books.google.at/books?id=s7vkBwAAQBAJ>
- [16] Mathuranathan, V.: *Simulation of Digital Communication Systems Using Matlab* [Kindle Edition], Amazon Digital Services, Inc, 2013, Retrieved from Amazon.com.
- [17] Maurer, L.; Haider, G.; Knapp, H.: 77 GHz SiGe based bipolar transceivers for automotive radar applications – An industrial perspective, in *2011 IEEE 9th Int. New Circuits and Systems Conf. (NEWCAS)*, 257–260.
- [18] Feger, R.; Pfeffer, C.; Scheibelhofer, W.; Schmid, C.M.; Lang, M.J.; Stelzer, A.: A 77-GHz cooperative radar system based on multi-channel FMCW stations for local positioning applications. *IEEE Trans. Microw. Theory Tech.*, **61** (1) (2013), 676–684.
- [19] Scheibelhofer, S.; Schuster, S.; Jahn, M.; Feger, R.; Stelzer, A.: Performance Analysis of Cooperative FMCW Radar Distance Measurement Systems, in *IEEE MTT-S Int. Microwave Symp. Digest 2008*, 121–124, June 2008.



Werner Scheibelhofer received the Dipl.-Ing. (M.Sc.) degree in mechatronics from the Johannes Kepler University, Linz, Austria, in 2009. In the same year, he joined the Institute for Communications Engineering and RF-Systems, Johannes Kepler University as Research Assistant. His research topics are radar system design and concepts for industrial radar sensors.



Reinhard Feger was born in Kufstein, Austria, in 1980. He received the Dipl.-Ing. (M.Sc.) degree in mechatronics and Dr. Techn. (Ph.D.) degree in mechatronics from Johannes Kepler University, Linz, Austria, in 2005 and 2010, respectively. In 2005, he joined the Institute for Communications and Information Engineering, Johannes Kepler University, as a Research Assistant. In 2007, he became a member of the Christian Doppler Laboratory for Integrated Radar Sensors, Johannes Kepler University. He is currently an Assistant Professor at the Institute for

Communications Engineering and RF-Systems, Johannes Kepler University. His research topics are radar signal processing, as well as radar system design for industrial and automotive radar sensors. Dr. Feger was recipient of the 2011 Microwave Prize and the 2011 German Microwave Conference Best Paper Award. In 2012, he received the Best Measurement Paper Prize at the European Conference on Antennas and Propagation.



Andreas Haderer received the Dipl.-Ing. (M.Sc.) degree in Communications Engineering from Technical University, Graz, Austria, in 2005. In the same year, he joined the Institute for Communications Engineering and RF-Systems, Johannes Kepler University as Research Assistant. His research topics are microwave imaging systems and

multidimensional radar-signal processing. He is co-founder of the Inras GmbH where he is responsible for the design of modern RF radar systems.



Stefan Scheiblhofer was born in Linz, Austria, in 1979. He received the Dipl.-Ing. (M.Sc.) degree in mechatronics and Dr. Techn. (Ph.D.) degree in mechatronics from Johannes Kepler University, Linz, Austria, in 2003 and 2007, respectively. Until 2010, he was with the Christian Doppler Laboratory for Integrated Radar Sensors, Institute

for Communications and Information Engineering, Johannes Kepler University. His primary research interests concern advanced radar system concepts, development of radar signal processing algorithms, statistical signal processing, RF design, and its application to automotive radar applications. Currently he is with Hainzl industrial systems in Linz.



Andreas Stelzer received the Diploma Engineer degree in Electrical Engineering from the Technical University of Vienna, Vienna, Austria, in 1994, and the Dr. Techn. degree (Ph.D.) in mechatronics (with honors sub auspiciis praesidentis rei publicae) from the Johannes Kepler University Linz, Austria, in 2000.

In 2003, he became Associate Professor with the Institute for Communications Engineering and RF Systems, Johannes Kepler University, Linz. Since 2008, he has been a key researcher for the Austrian Center of Competence in Mechatronics (ACCM), where he is responsible for numerous industrial projects. Since 2007, he has been head of the Christian Doppler Research Laboratory for Integrated Radar Sensors, and since 2011 he is a full Professor at the Johannes Kepler University, Linz, heading the Department for RF-Systems. He has authored or coauthored over 330 journal and conference papers. His research is focused on microwave sensor systems for industrial and automotive applications, radar concepts, SiGe-based circuit design, microwave packaging in eWLB, RF and microwave subsystems, surface acoustic wave (SAW) sensor systems and applications, as well as digital signal processing for sensor signal evaluation. Dr. Stelzer is a member of the Austrian ÖVE. He has served as an associate editor for the IEEE MICROWAVE AND WIRELESS COMPONENTS LETTERS. Currently he serves as Co-Chair for MTT-27 Wireless-Enabled Automotive and Vehicular Applications. He was the recipient of several awards, including the 2008 IEEE Microwave Theory and Techniques Society (IEEE MTT-S) Outstanding Young Engineer Award and the 2011 IEEE Microwave Prize. Furthermore, he was recipient of the 2012 European Conference on Antennas and Propagation (EuCAP) Best Measurement Paper Prize, the 2012 Asia Pacific Conference on Antennas and Propagation (APCAP) Best Paper Award, the 2011 German Microwave Conference (GeMiC) Best Paper Award, as well as the IEEE COM Innovation Award and the European Microwave Association (EuMA) Radar Prize of the European Radar Conference (EuRAD) 2003. He is a member of the IEEE MTT, IM, and CAS Societies and he serves as IEEE Distinguished Microwave Lecturer for the period 2014–2016.